



Fabrication of Dye Sensitized Solar Cell and Efficiency Enhancement by Using N719 and Z907 Dyes Mixture

Abdulrahman K. Ali¹, Nabeel A. Bakr^{2,*}, Shaimaa M. Jassim²

¹Department of Applied Science, University of Technology, Baghdad, Iraq

²Department of Physics, College of Science, University of Diyala, Diyala, Iraq

Email address:

nabeelalibakr@yahoo.com (N. A. Bakr), nabeelalibakr@sciences.uodiyala.edu.iq (N. A. Bakr)

*Corresponding author

To cite this article:

Abdulrahman K. Ali, Nabeel A. Bakr, Shaimaa M. Jassim. Fabrication of Dye Sensitized Solar Cell and Efficiency Enhancement by Using N719 and Z907 Dyes Mixture. *Journal of Photonic Materials and Technology*. Vol. 2, No. 3, 2016, pp. 20-24. doi: 10.11648/j.jpmt.20160203.11

Received: September 29, 2016; Accepted: October 17, 2016; Published: October 28, 2016

Abstract: This study aims to investigate the effect of N719 and Z907 dyes mixture (1:1 v/v ratio) on the DSSCs fabricated successfully using a simple procedure without the need for any complicated facilities. The XRD analysis of the TiO₂ layer confirmed that it has a polycrystalline structure belonging to anatase phase with crystallite size of 12.4 nm. UV-Vis spectroscopy was used to characterize the absorbance spectra of the TiO₂ layer, N719 dye, Z907 dye, dyes mixture and the fabricated DSSCs as well. The absorption spectra in the wavelength range of (350-750) nm show that the DSSC fabricated with dyes mixture has higher absorption compared to the other two cells. The dyes mixture performs better than the individual dyes due to the broadening of its UV-Vis spectrum in the blue region. The energy gap of the TiO₂ layer estimated by Tauc's plot was 3.12 eV. The SEM micrograph of the TiO₂ layer shows that the layer has a spongy shape with reduction in the number of open pores making easy for dye adsorption and electron transport. The average roughness, root mean square roughness and grain size of the TiO₂ layer estimated from the AFM micrograph and the granularity cumulative distribution chart were about 0.356 nm, 0.423 nm and 82.48 nm respectively. Solar cells with efficiency as high as 2.287% have been achieved using the dyes mixture as sensitizer which represents an enhancement of ~ 70% and ~ 106% compared to the DSSCs efficiencies prepared by N719 and Z907 dyes respectively.

Keywords: DSSC, N719 Dye, Z907 Dye, Dyes Mixture, Conversion Efficiency

1. Introduction

The increasing energy demand has been promoting the creation of devices that are able to convert alternative source of energy, such as solar energy [1]. Solar energy will play an important role in satisfying future energy needs of mankind since coal and natural reserves are being consumed at faster rates [2]. Dye sensitized solar cells (DSSCs) are photoelectrochemical, alternative energy source devices that convert light energy into electricity [3]. Since dye sensitized solar cells were first proposed by O'Regan and Grätzel in 1991, they have been attracting considerable attention because of their high efficiency, simple fabrication process and low production cost [4, 5]. The DSSC comprises a dye adsorbed nanocrystalline TiO₂ layer fabricated on a transparent conducting oxide (TCO) as the working

electrode, platinum (Pt) as the counter electrode, and an electrolyte solution with iodide/triiodide redox reagents [6] as shown in figure (1).

One of the major constituents, the sensitizing dye, plays a crucial role for efficient light harvesting and overall light to electricity conversion efficiency [2]. Therefore, we also provide analytical studies of DSSCs using two different dye sensitizers, i.e. N719 and Z907. The molecular structures of these dyes are shown in figure (2) [1]. Historically N719 is the most popular benchmark which served the seminal role in design and engineering of novel photosensitizers to achieve high extinction coefficient, long term stability, thiocyanate free photosensitizers for high efficiency and long term stability, cyclometalated Ru (II) dyes and photosensitizers for NIR response [7].

The most efficient DSSCs demonstrated to date have all been based on N719 dye developed by the Grätzel group. As

well as superior light harvesting properties and durability, a considerable advantage of these dyes lies in the metal-ligand charge transfer (MLCT) transition, through which the photoelectric charge is injected into the TiO_2 [8].

N719 dye achieved 11.3% conversion efficiency in DSSC [9]. Z907 has shown high performance in liquid electrolyte DSSCs. Z907, on the other hand, was selected as it has been widely studied as a sensitizer in DSSCs and achieves efficiencies of approximately 4% [10]. The Z907 dye, which has nonyl chains on one bipyridine ligand, is more effective in shielding the TiO_2 surface from the Co(III) approach, and has shown better performances than N719 in Co(II)/Co(III)-based DSSCs [11].

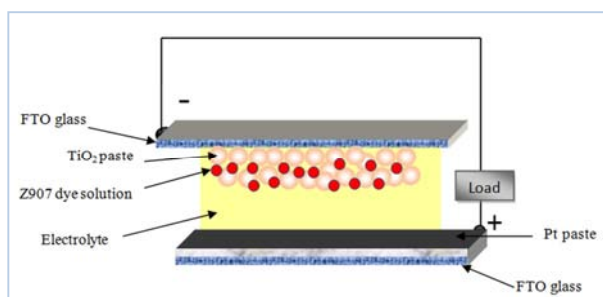


Fig. 1. Schematic diagram of DSSC basic structure.

In many studies single dye was employed as a light absorbing unit. The disadvantage of using a single dye is that the dye works in a narrow range of solar spectrum, which would minimize the cell efficiency.

It has been reported that the use of several dyes with complementary absorption spectra would broaden the spectral sensitivity of the cell, resulting in higher conversion efficiency [12].

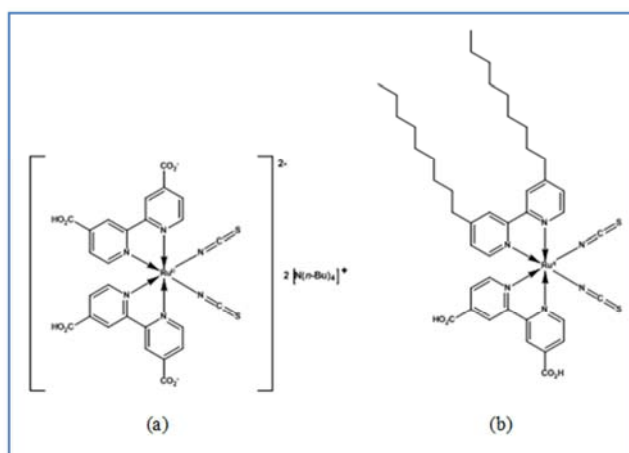


Fig. 2. Molecular complexes of Ruthenium based dye: (a) N719, and (b) Z907 [11].

The aim of this work is to prepare a dye sensitized solar cell using a simple procedure without the need for complicated facilities and to investigate the effect of dyes mixture on the power conversion efficiency (η) of the prepared solar cell.

2. Experimental Procedure

All the materials used in this work were supplied by Dyesol Company/Australia. The materials were as follows: Fluorine Tin Oxide (FTO) (resistance $8 \Omega/\text{sq}$) coated glass substrates, TiO_2 paste (18-NRT), Z907 dye, N719 dye, organic solvent based electrolyte (EL-HSE), platinum paste, sealing material, Acetone, distilled water.

For the preparation of the working electrode, FTO glass substrate with size of ($2.5 \text{ cm} \times 2.5 \text{ cm}$) was used. The FTO glass was cleaned in ultrasonic bath for 5 minutes in distilled water and for 5 minutes in acetone. The TiO_2 paste was deposited on FTO glass by Doctor-blade method and the thickness of the titania layer was determined by the thickness of scotch tape which has a thickness of $10 \mu\text{m}$ placed on the right and left sides of the conductive face of substrate. Then the scotch tape was removed and the films were left to dry for 30 minutes in a covered Petri dish. Thereafter, the films were annealed at 550°C for 30 minutes in ambient atmosphere. Finally, the working electrodes were allowed to cool at room temperature. After cooling, the working electrodes were immersed in a 0.25 mM N719 dye solution for 24 hours. This procedure was repeated for the electrodes with Z907 and dyes mixture (N719 and Z907, 1:1 v/v ratio). For the preparation of the counter electrode, two holes of 1 mm diameter were drilled to enable a later injection of electrolyte and platinum (Pt) paste was deposited on conductive side of FTO glass by Doctor-blade method, and the electrodes were then annealed at 450°C for 30 minutes in ambient atmosphere. This leads to homogenous distributed platinum with good catalytic activity.

The working electrode and counter electrode were assembled into a sandwich structure using sealant gasket, with a thickness of $30 \mu\text{m}$ as spacer. The sealant gasket was placed around TiO_2 paste and the counter electrode was put on it while the Pt film faces the TiO_2 . Finally, few drops of the electrolyte were injected through the holes in the counter electrode by a pipette, and the holes were sealed by plaster to prevent evaporation.

The crystallite phase of TiO_2 was identified by X-ray diffractometer (Shimadzu 6000, Japan) using $\text{CuK}\alpha$ radiation ($\lambda = 1.5406 \text{ \AA}$). The surface morphology of TiO_2 was investigated by SEM (JSM-7000F) type. The UV-Vis absorption spectra of the TiO_2 layer, Z907 dye, N719 dye, dyes mixture and DSSCs, were measured by UV-VIS-NIR spectrophotometer (Shimadzu, UV-1800). The photovoltaic performance of the DSSCs was measured using Keithley 2400 multimeter and tungsten halogen lamp. Based on I-V curve, the fill factor (FF) was calculated according to the formula:

$$\text{FF} = \frac{J_{\text{max}} \cdot V_{\text{max}}}{J_{\text{sc}} \cdot V_{\text{oc}}} \quad (1)$$

Where J_{max} is the maximum photocurrent density, V_{max} is maximum photovoltage, J_{sc} is the short circuit photocurrent density and V_{oc} is the open-circuit photovoltage. The photoelectric conversion efficiency (η) was calculated

according to the following equation:

$$\eta(\%) = \frac{J_{sc} \cdot V_{oc} \cdot FF}{P_{in}} \times 100 \quad (2)$$

Where P_{in} is the incident power.

3. Results and Discussion

3.1. Structural Analysis

Crystalline characterizations of TiO_2 film prepared by Doctor-blade technique on glass substrate were carried out by X-ray diffraction (XRD). Figure (3) shows the XRD diffraction pattern of the TiO_2 film annealed at 550 °C. From the figure, it was confirmed that the TiO_2 layer material has anatase phase with polycrystalline structure according to the ICDD standard card no. (21-1272) [13]. The diffraction peaks were indexed to the crystal planes (101), (004), (200), (105), (211), (204) and (215) and this result is in agreement with the results reported by Wang et al. [14]. The highest and strongest peak of TiO_2 thin film was at $2\theta \approx 25.4^\circ$ corresponding to (101) direction. The crystallite size of TiO_2 film was calculated by Scherrer's formula given by the following equation [15]:

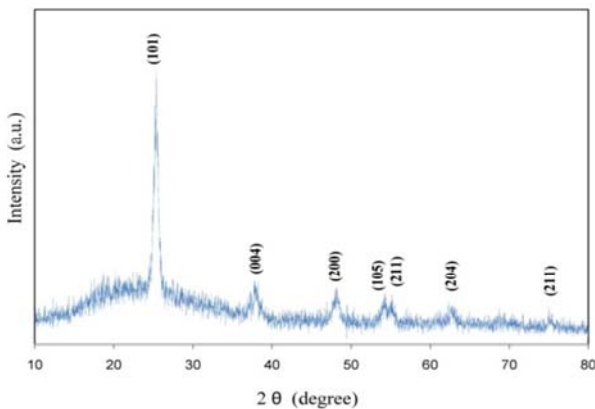


Fig. 3. XRD patterns of TiO_2 thin film.

$$D = 0.9 \lambda / \beta \cos\theta \quad (3)$$

Where D is the crystallite size, λ is the X-ray wavelength of $Cu K\alpha$ radiation, β is the full width at half maximum (FWHM) and θ is the Bragg's angle. The lattice parameters of the TiO_2 film are $a = 3.781 \text{ \AA}$ and $c = 9.477 \text{ \AA}$, which are in agreement with the standard values (i.e., $a = 3.785 \text{ \AA}$ and $c = 9.513 \text{ \AA}$) and the crystallite size is 12.4 nm.

3.2. Morphological Analysis

The surface morphology of TiO_2 thin film was characterized by SEM. Figure (4) displays the SEM image of TiO_2 film of 10 μm thickness which has been deposited on the FTO glass after annealing at 550 °C for 30 minutes. The SEM micrograph shows a spongy shape with reduction in the number of open pores making easy for dye adsorption and electron transport [16]. The average particle size of TiO_2 NPs is about 20-40 nm. The small particles of TiO_2 film have

larger surface area and subsequently absorb more dye molecules and this may lead to improved DSSC performance.

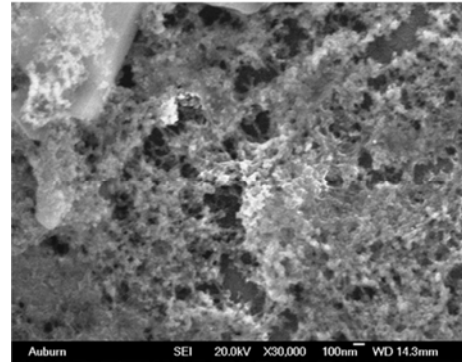


Fig. 4. SEM image of TiO_2 thin film at 30,000X.

3.3. (AFM) Results

The surface topography of TiO_2 film prepared by Doctor-blade method on FTO glass was studied by Atomic Force Microscope (AFM) technique. The 3-D AFM image and granularity cumulative distribution chart of TiO_2 film annealed at 550°C for 30 minutes are shown in figures (5a) and (4b) respectively. The average roughness, root mean square roughness and grain size of the TiO_2 film were about 0.356 nm, 0.423 nm and 82.48 nm respectively.

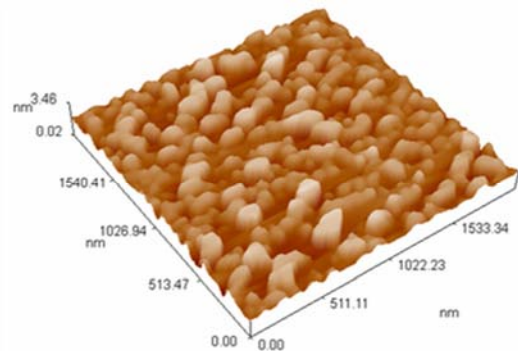


Fig. 5a. 3-D AFM image of TiO_2 thin film.

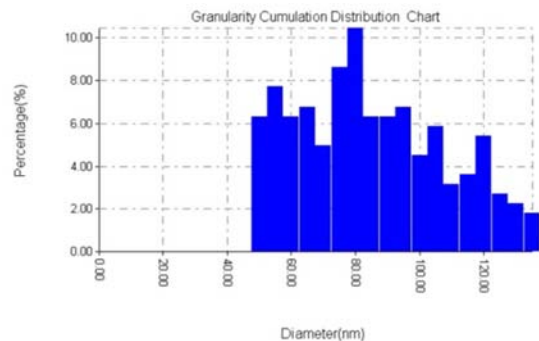


Fig. 5b. Granularity Cumulative Distribution chart of TiO_2 thin film.

3.4. Optical Properties

Figure (6) illustrates the UV-Vis absorption spectrum of

TiO₂ film annealed at 550°C. From the figure, it can be noticed that the film has clear and sharp absorption edge at wavelength of ~ 350 nm.

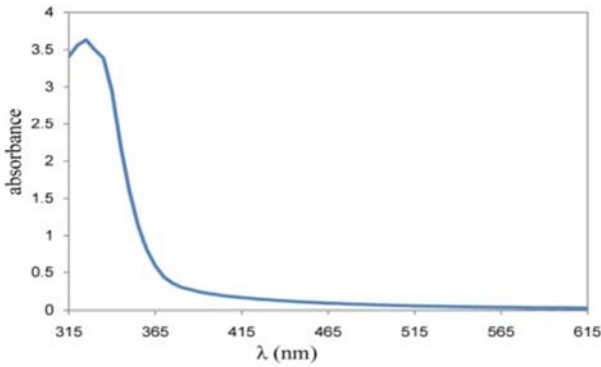


Fig. 6. UV-Vis absorbance of TiO₂ film.

The direct band gap of the TiO₂ thin film was determined by plotting $(\alpha h\nu)^2$ vs. $h\nu$. The optical band gap E_g value is estimated by extrapolation of the straight-line portion of the plot to zero absorption edge as shown in Figure (7). From the figure, it was observed that direct optical band gap for annealed TiO₂ thin film was 3.12 eV.

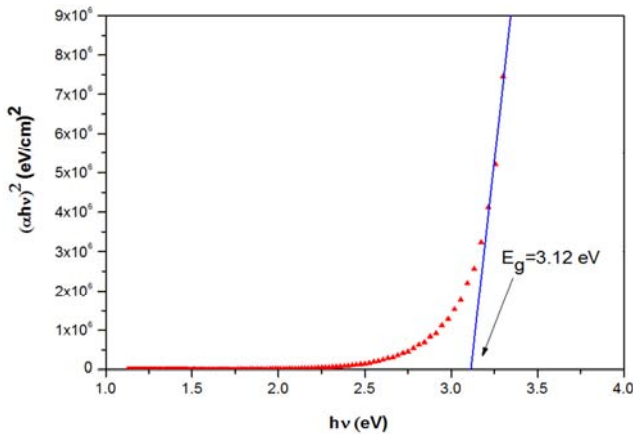


Fig. 7. Tauc's plot of TiO₂ film.

Figure (8) demonstrates the absorption spectra of N719, Z907 and their mixed solutions (1:1 v/v ratio) in the wavelength range of (350-800) nm. The UV-Vis absorption spectra show two absorption peaks at around (386 and 526), (426 and 532), and (396 and 536) nm, for N719, Z907 dyes and their mixed solutions respectively. It can be also observed that the N719 dye shows the highest absorption, while Z907 dye shows the lowest absorption.

The absorption spectra of DSSCs using N719, Z907 dyes and their mixture in the wavelength of 350-750 nm are shown in figure (9). From the absorption spectra, it can be seen that DSSC with mixture dye has higher absorption compared to the other two cells. Due to the enhancement in absorption, one may expect certain enhancement in efficiency.

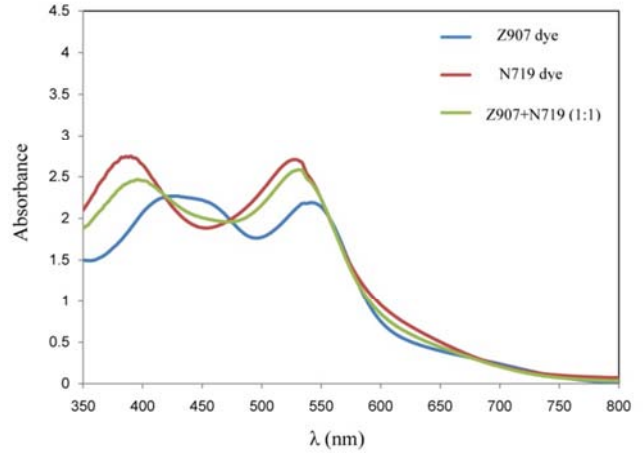


Fig. 8. UV-Vis absorbance of N719, Z907 dyes and their mixed solutions (N719 + Z907, 1:1 v/v ratio).

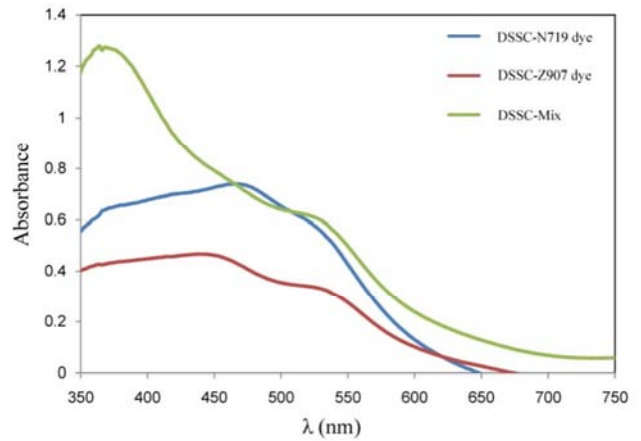


Fig. 9. UV-Vis absorbance of DSSCs.

3.5. Current Voltage Characteristics

Figure (10) illustrates the J-V characteristics of the DSSCs sensitized with N719, Z907 and dyes mixture (N719+Z907, 1:1 v/v ratio). It is clear that DSSC sensitized with dyes mixture shows J_{SC} , V_{OC} and the area of the J-V curve are the highest compared with DSSCs prepared using individual dyes indicating that this cell generates the highest output power. The photovoltaic parameters of all solar cells prepared in this study are summarized in Table 1.

The dyes mixture was expected to perform better than the individual dyes due to the broadening of its UV-Vis spectrum in the blue region [3]. This indicates that mixed co-sensitization of the two dyes could effectively transfer energy in a cooperative manner to the TiO₂ semiconductor resulting in an enhancement of the photovoltaic parameters of the cell [17]. The efficiency of the DSSC prepared by the dyes mixture as sensitizer enhanced ~ 70% and ~ 106% compared to the DSSCs prepared by N719 and Z907 dyes respectively.

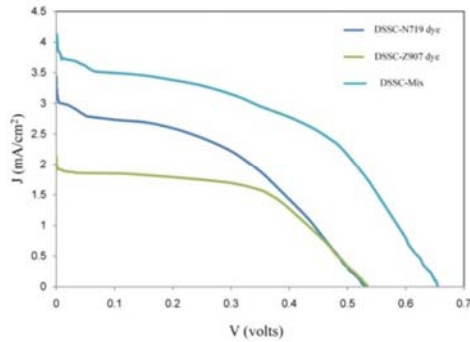


Fig. 10. *J-V* curves of DSSCs using N719, Z907 and their mixed solutions (N719 + Z907, 1:1 v/v ratio).

Table 1. The photovoltaic parameters of DSSCs fabricated using N719, Z907, and their mixed solutions (N719 + Z907, 1:1 v/v ratio).

DSSC sensitizer	V_{oc} (V)	J_{sc} (mA/cm ²)	V_{max} (V)	J_{max} (mA/cm ²)	FF	η (%)
N719	0.535	3.429	0.323	2.079	0.366	1.343
Z907	0.535	2.135	0.360	1.539	0.485	1.108
Mix	0.655	4.132	0.44	2.599	0.422	2.287

4. Conclusions

DSSCs with N719, Z907 dyes and their mixture (1:1 v/v ratio) have been fabricated successfully using a simple procedure without the need for any complicated facilities. The absorption spectra in the wavelength range of (350–750) nm show that the DSSC fabricated with dyes mixture has higher absorption compared to the other two cells. The dyes mixture performs better than the individual dyes due to the broadening of its UV-Vis spectrum in the blue region. This indicates that the mixed co-sensitization of the two dyes could effectively transfer energy in a cooperative manner to the TiO₂ semiconductor resulting in an enhancement of the photovoltaic parameters of the cell. The efficiency of the DSSC prepared with the dyes mixture as sensitizer was 2.287% which represents an enhancement of ~ 70% and ~ 106% compared to the DSSCs efficiencies prepared by N719 and Z907 dyes respectively.

References

- [1] N. M. Nursama and L. Muliani, "Investigation of photoelectrode materials influences in titania-based-dye sensitized solar cells", *International Journal of Technology*, Vol. 2, pp.129-139, (2012).
- [2] T. G. Deepak, G. S. Anjusree, K. N. Pai, D. Subash, S. V. Nair, and A. S. Nair, "Fabrication of a dye-sensitized solar cell module using spray pyrolysis deposition of a TiO₂ colloid", *RSC Advances*, Vol. 4, pp. 23299–23303, (2014).
- [3] A. Lim, N. Haji Manaf, K. Tennakoon, R. L. N. Chandrakanthi, L. B. L. Lim, J. M. R. S. Bandara, and P. Ekanayake, "Higher Performance of DSSC with Dyes from *Cladophora* sp. as Mixed Cosensitizer through Synergistic Effect", *Journal of Biophysics*, Vol. 2015, ID 510467, pp.1-8, (2015).
- [4] K. Guo, M. Li, X. Fang, X. Liu, B. Sebo, Y. Zhu, Z. Hu, and X. Zhao, "Preparation and enhanced properties of dye-sensitized solar cells by surface plasmon resonance of Ag nanoparticles in nanocomposite photoanode", *Journal of Power Sources*, Vol. 230, pp. 155-160, (2013).
- [5] T. Y. Lee, P. S. Alegaonkar, and J. B. Yoo, "Fabrication of dye sensitized solar cell using TiO₂ coated carbon nanotubes", *Thin Solid Films*, Vol. 515, pp. 5131–5135, (2007).
- [6] S. N. Karthick, K. V. Hemalatha, C. J. Raj, H. J. Kim, and Y. Moonsuk, "Titanium dioxide paste preparation for dye sensitized solar cell using hydrothermal technique", *Journal of Ceramic Processing Research*, Vol. 13, pp.136-139, (2012).
- [7] H. Cheema, A. Islam, L. Han, and A. El-Shafei, "Monodentate pyrazole as a replacement of labile NCS for Ru (II) photosensitizers: Minimum electron injection free energy for dye-sensitized solar cells", *Dyes and Pigments*, Vol. 120, pp. 93-98, (2015).
- [8] M. Gratzel, "Progress in Ruthenium Complexes for Dye Sensitized Solar Cells", *Platinum Metals Rev.*, Vol. 53, No. 4, pp. 216–218, (2009).
- [9] I. C. Berkman, "Investigation of the electronic structure of the ruthenium dyes used in solar cells by combining hartree-fock theory with the quantum monte carlo technique", MSc. Thesis, (2015).
- [10] G. Y. Margulis, B. E. Hardin, I. K. Ding, E. T. Hoke, and M. D. McGehee, "Parasitic Absorption and Internal Quantum Efficiency Measurements of Solid-State Dye Sensitized Solar Cells", *Adv. Energy Mater*, Vol. 3, pp. 959–966, (2013).
- [11] Paolo Salvatori, Gabriele Marotta, Antonio Cinti, Chiara Anselmi, Edoardo Mosconi, and Filippo De Angelis, "Supramolecular Interactions of Chenodeoxycholic Acid Increase the Efficiency of Dye-Sensitized Solar Cells Based on a Cobalt Electrolyte", *Journal of Physical Chemistry C*, Vol. 117, pp. 3874-3887, (2013).
- [12] J. Bandara and H. Weerasinghe, "Design of high-efficiency solid-state dye sensitized solar cells using coupled dye mixtures", *Solar Energy Materials & Solar Cells*, Vol. 90, pp. 864–871, (2006).
- [13] R. Vijayalakshmi and V. Rajendran, "Synthesis and characterization of nano-TiO₂ via different methods", *Archives of Applied Science Research*, Vol. 4 (2), pp. 1183-1190, (2012).
- [14] Y. Wang, L. Li, X. Huang, Q. Lia and G. Li, "New insights into fluorinated TiO₂ (brookite, anatase and rutile) nanoparticles as efficient photocatalytic redox catalysts", *RSC Advances*, Vol. 5 (43), pp. 34302-34313, (2015).
- [15] C. H. Wei and C. M. Chang, "Polycrystalline TiO₂ thin films with different thicknesses deposited on unheated substrates using RF magnetron sputtering", *Materials Transactions*, Vol. 52 (3), pp. 554-559, (2011).
- [16] H. Sh. Wu, and Y. L. Wang, "Effects of annealing temperature on the structure and properties of TiO₂ nanofilm materials", *Advanced Materials Research*, Vol. 531, pp. 203-206, (2012).
- [17] R. Tagliaferro, D. Colonna, T. M. Brown, A. Reale, and A. D. Carlo, "Interplay between transparency and efficiency in dye sensitized solar cells", *Optics express*, Vol. 21 (3), pp. 3235-3242, (2013).